Influence of morphology of low-band-gap PCDTBT:PC$_{71}$BM composite on photoinduced charge transfer: LEPR spectroscopy study

V.I. Krinichnyi*, E.I. Yudanova

Department of Kinetics and Catalysis, Institute of Problems of Chemical Physics RAS, Academician Semenov Avenue 1, Chernogolovka 142432, Russia

ABSTRACT

Light-induced electron paramagnetic resonance (LEPR) study the steady-state of spin charge carriers initiated by Vis-NIR irradiation with the energy (wavelength) of 1.32–2.73 eV (940–455 nm) in organic composite of a low-band-gap poly(*N*-9′-heptadecanyl-2,7-carbazole-alt-5,5-(4′,7′-di-2-thienyl-2′,1′,3′-benzothiadiazole)) (PCDTBT) with a [6,6]-phenyl-C$_{71}$-butyric acid methyl ester (PC$_{71}$BM) within a wide temperature range is reported. LEPR spectra of the PCDTBT:PC$_{71}$BM composite were deconvoluted and the main resonance parameters of polarons and anion radicals of methanofullerene were determined. The reversible formation of spin traps in polymer backbone, whose number, distribution and depth governed by the photon energy, has being shown. A part of photoinduced charge carriers is pinned by such traps resulting in formation of domains with different band gaps and photon sensitivity. Relaxation and dynamics parameters of all the charge carriers determined separately by the steady-state saturation method were shown to depend extremely on the energy of exciting photons. Polaron diffusion along polymer chains was analyzed in terms of spin interaction with the lattice phonons of crystalline domains embedded into amorphous polymer matrix. Activation of polaron hopping over the energetic barrier is characteristic for the charge transfer between polymer chains. Small-angle librations of methanofullerene cages in the polymer matrix were shown to follow the Markus model. Our results suggest that C$_{70}$-counter-ions embedded into the PCDTBT backbone strengthen an overlapping of molecular orbitals and provoke a layered morphology of appropriate composite. This regularizes the polymer matrix, hinders the formation of spin traps and accelerates spin dynamics that in turn facilitates charge transport through bulk heterojunctions. It was shown that the spin-assisted photon-electron conversion is realized in the composite within the visible and near-infrared range of the sun spectrum with comparable efficiency.

© 2015 Elsevier B.V. All rights reserved.

1. Introduction

The discovery of the photovoltaic effect in organic composite of an electron-donating conjugated polymer and an electron-accepting fullerene and its intensive study clearly demonstrated the formation of excitons upon light illumination. The exitons can be transformed into donor-acceptor complexes collapsing into radical pairs, namely positively charged polarons delocalized along polymer chains and negatively charged fullerene anion radicals embedded into polymer matrix [1]. This confirmed a disruption of strongly bound neutral excitons into spin-charge-carrying quasi-pairs on a picosecond time scale due to photoinduced electron hopping from the conjugated polymer to the fullerene cage. This effect can be used for the realization of low-

cost printable, portable and flexible renewable energy sources [2]. Previous research has mainly focused on bulk heterojunctions (BHJ) formed by conjugated polymers and fullerene derivatives. One key characteristic for such compounds is the nanophase separation between polymer and fullerene subsystems, which leads to a large interface for charge dissociation, and bicontinuous pathways for charge transport. The soluble poly(3-hexylthiophene) (P3HT) and [6,6]-phenyl-C$_{61}$-butyric acid methyl ester (PC$_{61}$BM) mainly used for such purposes as electron donor and acceptor, respectively, allowed to reach power conversion efficiency of 4–5% [3]. So small efficiency is explained by relatively large band gap of P3HT ($\sim$1.9 eV) limiting the fraction of the solar spectrum and the relatively small energy difference between the highest occupied molecular orbital (HOMO) of P3HT and the lowest unoccupied molecular orbital (LUMO) of PC$_{61}$BM. In order to improve the light power conversion efficiency, these energies defined by the polymer band gap and HOMO should be decreased.

* Corresponding author.
E-mail address: kivirus@gmail.com (V.I. Krinichnyi).

Recently, several low-band-gap co-polymers based on poly(2,7-carbazole) derivatives were developed to absorb the wider solar spectrum with deeper HOMO [4]. These polymers are characterized by the internal charge transfer from an electron-rich unit to an electron-deficient moiety within each repeating unit. Tuning of their light-absorption ability and energy levels foredoomed extensive development and study. Among them, poly[[9-(1-octylnonyl)-9H-carbazole-2,7-diyl]-2,5-thiophenediyl-2,1,3-benzothiadiazole-4,7-diyl-2,5-thiophenediyl] (PCDTBT) (see Fig. 1 for its molecular structure) with band gap near 1.88 eV [5] were discovered [6] to be one of the most efficient matrix for organic plastic field-effect transistors and solar cells [7]. Due to a relatively deep HOMO of active matrix and maximal internal quantum efficiency the light conversion efficiency of the PCDTBT:PC$_{71}$BM composite layer reached 6–7% recently [8]. The higher light absorbance is due to the lower spherical symmetry of the fullerene
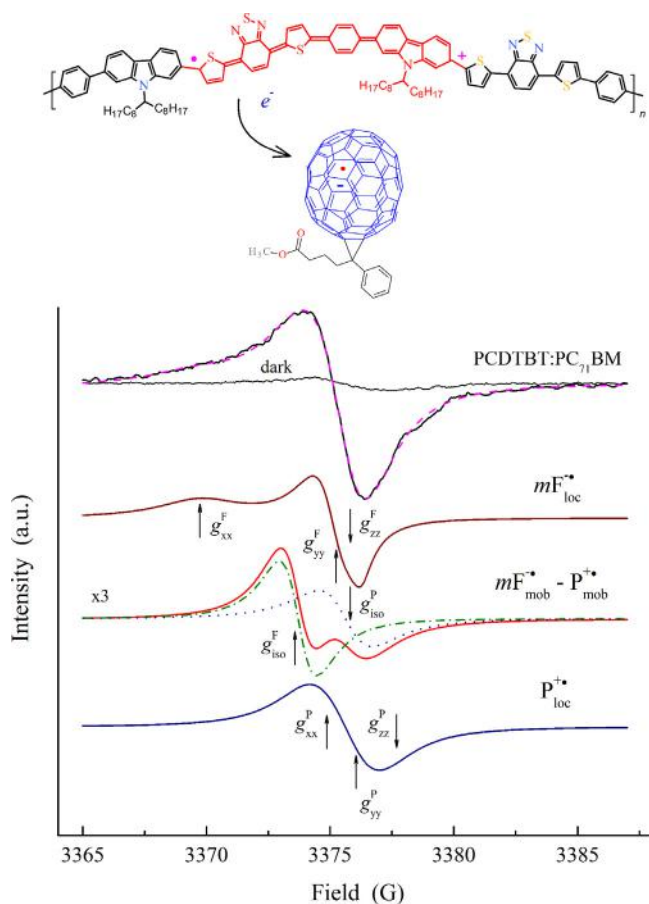
in PC$_{71}$BM cage as compared to PC$_{61}$BM globe in appropriate PCDTBT:PC$_{x1}$BM BHJ [9]. One, however, should note that the extended spectral range of absorption may be overbalanced by recombination losses, or alternatively, by wasteful triplet formation [10]. Higher efficiency was achieved mainly due to ultrafast charge separation in the PCDTBT:PC$_{71}$BM composite before localization of the primary excitation to form a bound exciton in contrast with conventional polymer:fullerene systems [11]. Besides, morphology of the PCDTBT:PC$_{71}$BM BHJ becomes laterally oriented with "column-like" bilayer ordered polymer backbone [12] that improves the intralayer carrier mobility. Higher π-overlaping in such two-dimensional polymer backbone hinders its torsional twisting and, therefore, decreases the energy of its band gap [13]. This also accelerates charge hopping along and between PCDTBT bilayers. This evidences that charge dynamics is another important parameter affecting device light conversion efficiency. An understanding of the charge separation, transport and recombination in such materials at a molecular level is crucial for the improving of the electronic properties and efficiency of appropriate molecular electronics. However, the link between the quantum efficiency, dynamics of charge carriers and energy of photons within the BHJ absorption spectrum is yet to be established.

Opposite charge carriers are characterized by spin $S = 1/2$, so their magnetic, relaxation and dynamic properties can be undoubtedly studied in details by inter alia light-induced electron paramagnetic resonance (LEPR) spectroscopy [2,14,15]. The method appeared to be a very efficient tool for the investigation of electronic transfers within BHJ on the molecular scale because it allows in situ detection of the paramagnetic species resulting from such transfers. LEPR measurements, especially at millimeter wavebands [16–18], revealed the existence of polarons and fullerene counter-ions with different line shapes, EPR parameters and saturation properties. The method in combination with the microwave (MW) power saturation method allowed detecting electron relaxation, lifetime [19] and recombination [20] of spin charge carriers in various polymer:fullerene systems. Niklas et al. determined [18] the main values of g-tensors, $g_{xx} = 2.0032$, $g_{yy} = 2.0024$, $g_{zz} = 2.0018$ for polarons and $g_{xx} = 2.0060$, $g_{yy} = 2.0028$, $g_{zz} = 2.0021$ by D-band (130 GHz) LEPR method for methanofullerene anion radicals photoinduced in the PCDTBT:PC$_{71}$BM composite at $T = 50$ K. A recombination of charge carriers was proved to be spin-dependent [21]. This means that their spin origin can play a key role in the controlling and handling of electronic properties of photovoltaic devices by the EPR spectroscopy. Composition, relaxation and dynamics of charge carriers photoinduced in organic semiconductors are governed by spin-dependent exciton-charge interactions and consistent with the model of spin-assisted recombination of polaron pairs [22]. So, the study of photoinitiated electronic processes in polymer:fullerene systems under spin resonance could to help us in creation of novel organic photovoltaic and spintronic devices. However, the dynamics and interaction of different spin ensembles affecting conversion efficiency of such and other polymer:fullerene BHJ are under debate and there not simple picture cleaning spin resonance-assisted processes in organic photoexcited systems.

It was shown by us that a part of polarons formed after exciton formation in result of irradiation of polymer backbone is pinned by spin traps whose the number and depth are governed by the composite morphology and photon energy [23,24]. Spin relaxation and charge carrier dynamics were shown to be governed by spin exchange and by the photon energy [23–26]. Formation, relaxation and dynamics of these charge carriers in the PCDTBT:PC$_{61}$BM BHJ were studied in wide photon energy and temperature ranges [27]. Essential LEPR response of this composite appeared to be registered upon its irradiation even by IR photons with the

Fig. 1. Dark and background irradiated by white light with the color temperature $T_c = 5500$ K at $T = 77$ K 3-cm waveband LEPR spectra of the PCDTBT:PC$_{71}$BM composite (1), attributed to localized methanofullerene anion radicals $mF_{loc}^{\bullet -}$ and polarons $P_{loc}^{\bullet +}$ as well as mobile radical quasi-pairs $P_{mob}^{\bullet +} - mF_{mob}^{\bullet -}$. The main values of their g-tensors, g_{ii}, and isotropic g-factors, g_{iso}, are shown as well. The spectrum calculated using $g_{iso}^P = 2.0024$ and $g_{iso}^{mF} = 2.0036$ determined from the fitting for $P_{mob}^{\bullet +}$ and $mF_{mob}^{\bullet -}$, respectively, fixed shifts $g_{iso}^P - g_{xx} = -7.3 \times 10^{-4}$, $g_{iso}^P - g_{yy} = 7.0 \times 10^{-5}$, $g_{iso}^P - g_{zz} = 6.7 \times 10^{-4}$, $g_{iso}^{mF} - g_{xx} = -2.37 \times 10^{-3}$, $g_{iso}^{mF} - g_{yy} = 8.3 \times 10^{-4}$, $g_{iso}^{mF} - g_{zz} = 1.53 \times 10^{-3}$, determined at D-band EPR for $P_{loc}^{\bullet +}$ and $mF_{loc}^{\bullet -}$, respectively, immobilized in the PCDTBT:PC$_{71}$BM BHJ (see the text), and concentration ratio for these charge carriers $[P_{loc}^{\bullet +}]:[P_{mob}^{\bullet +}]:[mF_{loc}^{\bullet -}]:[mF_{mob}^{\bullet -}] = 1.00:1.39:2.37:1.39$ is shown by dashed line. Spectral terms calculated for $P_{mob}^{\bullet +}$ and $mF_{mob}^{\bullet -}$ are shown by dotted and dash-dotted lines, respectively. At the top, the formation of polaron and methanofullerene charge carriers accompanying by the transfer of an electron from PCDTBT chain to PC$_{71}$BM cage is also shown schematically. It should be noted that a polaron is normally delocalized on nearly three PCDTBT units.

energy/wavelength of 1.32 eV/940 nm, in the absence of absorption where the optical absorption band is reset. This means that the spin concentration in the sample does not correlate definitely with the number of optical quanta absorbed by the sample. This observation is in contradiction with the conclusion made by Tong et al. [28] that the efficiency of carrier initiation in the fullerene-modified PCDTBT should be essentially independent of the excitation photon energy within sun spectrum range.

Here, we use direct LEPR spectroscopy combined with the MW steady-state saturation method to study the magnetic, relaxation and electronic properties of charge separated states of the PCDTBT:PC$_{71}$BM BHJ upon wider range of IR-Vis illumination. It demonstrated that the use of the PC$_{71}$BM counterions instead of the PC$_{61}$BM ones in appropriate composite leads to the arrangement of polymer matrix that increases its planarity, decreases the number of spin traps and, therefore, accelerates charge transfer through BHJ. The composite with PCDTBT matrix was confirmed to converse photons not only of visible light but also of infrared irradiation.

2. Experimental details

Poly[N-9′-heptadecanyl-2,7-carbazole-alt-5,5-(4′,7′-di-2-thienyl-2′,1′,3′-benzothiadiazole)] (PCDTBT) from the St. Jean Photochemicals Inc. and 99.5% [6,6]-phenyl-C$_{71}$-butyric acid methyl ester (PC$_{71}$BM) obtained from Solenne BV were used without further purification. Insert in Fig. 1 shows schematically chemical structures of these ingredients. First 0.7 mg of PCDTBT was dissolved in 0.5 ml of chlorbenzene:di-chlorbenzene (3:1) mixture. This solution was sonicated for 5 min in ultrasonic bath LT-05C (60 W) followed by heating at T = 333 K for 5 min. Fullerene derivative was added into above solution to the molar ratio PCDTBT:PC$_{71}$BM = 1:4, afterwards the resulting solution was additionally maintained at T = 333 K for 20 h to complete dissolution of PC$_{71}$BM. The prepared solution was serially casted onto both sites of ceramic plate and dried until polymer:fullerene composite was formed as double-sided film, both with the size of ca. $8 \times 4 \times 0.1$ mm^3.

The sample was permanently irradiated by the solid-state polychromic LXHL-LW3C (white, color temperature T_c = 5500 K, 5800 lx) and monochromic YT-5WIR850-H (1.32 eV/940 nm, 860 lx), HH-5WP2TR8502112-M-P (1.46 eV/850 nm, 1160 lx), HH-5WP2TR7702112-M-P (1.61 eV/770 nm, 1280 lx), HH-5WP2XR2112-T-P (1.91 eV/650 nm, 1180 lx), LXHL-LD3C (1.98 eV/625 nm, 5150 lx), LXHL-LL3C (2.10 eV/590 nm, 2500 lx), LXHL-LM3C (2.34 eV/530 nm, 3130 lx), LXHL-LE3C (2.46 eV/505 nm, 6200 lx), HH-5WP2AG2112-T-P (2.53 eV/490 nm, 6000 lx), LXHL-LR3C (2.73 eV/455 nm, 6150 lx) LED light sources with a spectral half bandwidth of ca. 15 nm/0.1 eV directly in the MW cavity through quartz light guide. Integral luminance I (lx) of these sources was estimated using a broadband IMO-2N output power light irradiation bolometer in combination with a digital luxmeter LX1010BS for the further normalization of spin concentration. In order to decompose overlapping signals for more precise estimation of their parameters, the "light on-light off" method with subsequent annealing was applied.

EPR measurements were performed using an X-band (3-cm, 9.7 GHz) PS-100X spectrometer with maximal MW power of 150 mW and 100 kHz field ac modulation for phase-lock detection. The former allowed reaching magnetic term B_1 of MW field up to 0.48 G. "Dark" and photoinduced EPR spectra of the composite were obtained at 77 K in quartz Dewar filled with liquid nitrogen and at 90–340 K in dry nitrogen flow using a BRT SKB IOH temperature controller. In the latter case, the temperature is controlled by calibrated Cu/Cu:Fe thermocouple with high sensitivity (15 μV/K at 20 K) and stability (0.5 K) situated around

the sample. Gaseous nitrogen flow with the stability of 0.1% makes it possible to vary temperature in the EPR cavity center with the error of 0.3 K. All the spectra were recorded under the same gain, modulation, accumulation times, accumulation number, and microwave power. The signal-to-noise ratio of the LEPR spectra was improved by signal averaging at several (typical 4–6) acquisitions. The number of all paramagnetic centers stabilized and photoinitiated in the composite was determined using comparable double integration of their contributions accurately deconvoluted from effective LEPR spectra and that of 2,2,6,6-tetramethylpiperidine-1-oxyl (TEMPO) nitroxide radical registered far from their MW saturation when the value of B_1 and amplitude of ac modulation B_m in the cavity center did not exceed 0.05 and 1.0 G, respectively. Operating conditions were chosen to avoid significant power saturation and modulation broadening, whereas electron relaxation parameters of both type charge carriers were determined separately using the steady-state saturation method [29] at $B_1 \leq 0.48$ G. Processing and simulations of the EPR spectra were performed with the Bruker SimFonia and OriginLab softwares. The error of determination of the spectral amplitude, width and position does not exceed ±3.8%, ±1.2, and ±0.11%.

3. Results and discussions

3.1. Spin composition and EPR parameters

Fig. 1 exhibits EPR spectra of the PCDTBT:PC$_{71}$BM composite obtained with and without background irradiation by polychromic (white, T_c = 5500 K) light at T = 77 K directly in the cavity of EPR spectrometer. Normally, polymer:fullerene samples in the dark demonstrate weak single EPR spectra attributed to intrinsic paramagnetic defects. Dark EPR spectrum of the composite under study presented in Fig. 1 could be also originated from the interaction with IR photons inside the spectrometer (see below). LEPR spectra consist of lines contributed from paramagnetic centers with different concentration, mobility and EPR parameters.

PCDTBT contains of some S and N heteroatoms with perceptible nuclear magnetic moment and, therefore, characterizing by different hyperfine constant. Weak spin-orbit interaction of an unpaired electron delocalized on a polaron with such heteroatoms has been detected by the high-field EPR spectroscopy [30] to provoke rhombic symmetry of spin density and, therefore, anisotropic g-factor and line width. Since the backbone of a conjugated polymer is preferably parallel to the film substrate [3], the lowest principal g-value, g_{zz}, is normally associated with the polymer backbone. The macromolecule can take any orientation relative to the z-axis, i.e., the polymer backbone direction is derived from the presence of both the g_{xx} and g_{yy} components in the spectra for all BHJ orientations in the sample. Thus, the g-factor anisotropy is a result of inhomogeneous distribution of additional fields along the x and y directions within the plane of the polymer σ-skeleton rather than along its perpendicular z direction. This parameter is governed by the structure and morphology of polymer matrix, hyperfine interaction of a polaron spin with a heteroatom nuclear, etc. EPR parameters of a fullerene anion radical are also weakly anisotropic. However, in contrast with a polaron, unpaired electron is localized rather on its C$_{xO}$-cage and weakly interacts with side groups [17]. If these spins move in condensed media these parameters are averaged shifting to an effective (isotropic) g-factor, $g_{iso} = (g_{xx} + g_{yy} + g_{zz})/3$. The line width of these charge carriers is also averaged similarly.

In order to obtain and analyze these parameters, one should deconvolute such spectra using the "light on-light off" procedure [17,18,24]. Each light photon initiates a priori a pair of opposite mobile charge carriers with averaged magnetic parameters. The part of these carriers is captured by spin traps, so the anisotropy of

their LEPR spectra becomes more obvious. Under these assumptions using the main values of **g**-tensors determined for charge carriers initiated in the PCDTBT:PC$_{71}$BM at 130 GHz waveband EPR by laser photons with the energy/wavelength of 2.33 eV/532 nm [18], one can obtain separately their magnetic resonance, relaxation and dynamics parameters. So, experimental LEPR spectra of the system under study as in the case of other PC$_{71}$BM-based polymer composites [17,18,24] were assigned to mobile radical quasi-pairs of the positively charged polarons $P_{mob}^{\bullet+}$ moving along polymer chains and methanofullerene anion radicals $mF_{mob}^{\bullet-}$ pseudo-rotating around own main molecular axis within polymer matrix as well as respective paramagnetic centers, $P_{loc}^{\bullet+}$ and $mF_{loc}^{\bullet-}$, captured by spin traps reversibly photoinduced in this matrix. Spectral contributions of these spins are also presented in Fig. 1. All terms of the sum spectra were analyzed to be characterized by Lorentzian line shape. As in the case of the P3HT:PC$_{61}$BM [23,31] and PCDTBT:PC$_{61}$BM [27] composites this argues in favor of a smaller number of spin traps and faster spin dynamics in the sample under study.

Normally, photoinitiation of such charge carriers occurs in the femtosecond time scale, whereas electron back transfer with charge annihilation is much slower due to relatively fast dynamics and slow structural relaxation in such a system [32]. This is the reason why an effective number of spin charge carriers should inversely depend on the probability of their recombination. Such process is determined by spin multistage activation diffusion along a polymer chain and tunneling from a chain to a fullerene anion [33]. The decay of mobile charge carriers photoinitiated in a polymer:fullerene system consists of temperature-independent fast and exponentially temperature-dependent slow contributions [23,26,34]. These processes are respectively ascribed to bimolecular recombination of mobile and less-mobile charge carriers trapped in deeper states [35]. As in case of PCDTBT:PC$_{61}$BM BHJ [27], the illumination of the composite under study, however, leads to drastic decrease in spin concentration in its BHJ. This can evidence for lower concentration of spin traps in this matrix that can also improve the electronic properties of this system.

3.2. Spin concentration

Effective concentration of all spins photoinduced in the PCDTBT:PC$_{71}$BM BHJ under permanent illumination by white light was determined to be $N = 3.3 \times 10^{19}$ spin/g at $T = 77$ K. This value is ~3 smaller than determined for PCDTBT:PC$_{61}$BM composite at similar experimental conditions [27]. This fact may indicate, e.g., the formation of a smaller number of trapped charge carriers and their faster recombination in the system under study. Because spin concentration is a function of spin traps [35], the number of charge carriers depends on the energy of initiating photons $h\nu_{ph}$ as it is shown in Fig. 2a. This can be explained by the reversible formation of spin traps in polymer matrix upon light illumination. The number, depth and distribution of such traps were shown [24,27] to depend on the structure of polymer matrix and energy of the light photons. It is seen from Fig. 2a, that a more significant change of spin concentration with a frequency occurs for mobile quasi-pairs $P_{mob}^{\bullet+}-mF_{mob}^{\bullet-}$. Rather drastic dependence of spin number on the photon energy is registered for photon of visible light band at $h\nu_{ph}/\lambda_{ph} \approx 2.7$ eV/460 nm lying around characteristic peaks registered in both the optical and photon-to-current efficiency spectra of morphologically optimized PCDTBT:PC$_{71}$BM films [28,36].

Two main features should be noticed from an analysis of the data presented. One of them is the initiation of spin charge carriers not only by photons of visible light (whose right sub-bands are restricted by horizontal dashed segments) but also by IR phonons (left sub-band) similarly to that as it was detected in case of the PCDTBT:PC$_{61}$BM system [27]. Thus, one can conclude that the weak spectrum obtained in the absence of light irradiation and shown in Fig. 1 might be attributed to the same paramagnetic centers
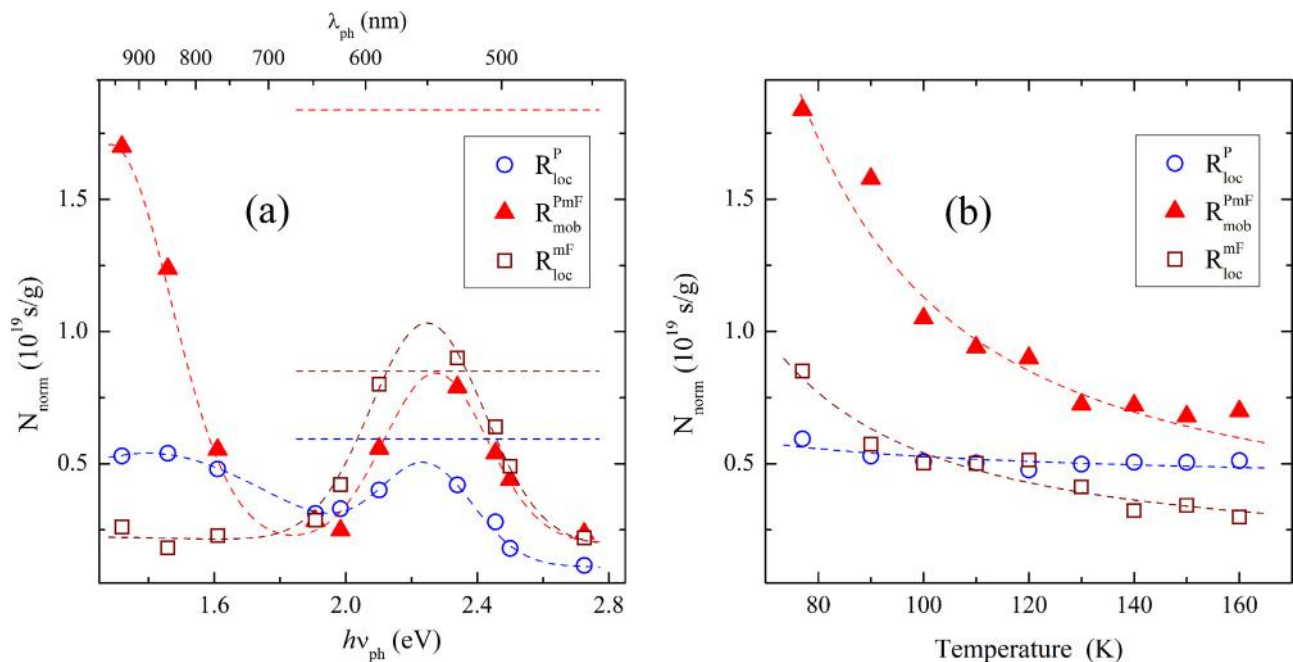

Fig. 2. (a) The concentration of immobilized charge carriers $P_{loc}^{\bullet+}$, $mF_{loc}^{\bullet-}$ and mobile quasi-pairs $P_{mob}^{\bullet+}-mF_{mob}^{\bullet-}$ photoinduced in the PCDTBT:PC$_{71}$BM composite at $T = 77$ K as a function of photon energy $h\nu_{ph}$ (wavelength λ_{ph}) normalized to illuminance I of light sources. Respective values determined for these centers initiated in the system by white light are shown by the bottom, middle and top horizontal dashed sectors, respectively. Dashed lines connecting the experimental points are painted arbitrarily only for illustration to guide the eye. (b) Temperature dependence of concentration of these charge carriers photoinduced in the composite by photons of white light with color temperature $T_c = 5500$ K. Up-to-down dashed lines show the dependences calculated from Eq. (1) with $\Delta E_{ij} = 0.015$, 0.002 and 0.012 eV, respectively.

Table 1

The peak-to-peak line width $\Delta B_{pp}^{(0)}$, spin-lattice $T1$ and spin–spin $T2$ relaxation times, and anisotropy of spin dynamics, $A = D_{1D}/D_{3D}$, determined for charge carriers induced in the PCDTBT:PC$_{71}$BM composite upon illuminated by photons with different energy $h\nu_{ph}$/wavelength λ_{ph} at $T = 77$ K.

Parameter	$h\nu_{ph}/\lambda_{ph}$, eV/nm										
	|White|	1.32/940	1.46/850	1.61/770	1.91/650	1.98/625	2.10/590	2.34/530	2.46/505	2.53/490	2.73/455
$\Delta B_{pp}^{(0)\text{a}}$, G	1.74	2.21	1.49	1.66	1.82	2.03	2.33	2.13	1.97	1.96	2.52
$\Delta B_{pp}^{(0)\text{b}}$, G	1.47	1.83	1.68	1.89	1.71	1.62	1.72	2.29	2.51	2.42	2.31
T_1^{Pc}, 10^- s	2.30	2.91	1.93	1.71	1.52	1.51	1.33	1.03	1.16	1.28	2.21
T_1^{mFd}, 10^{-6} s	0.67	0.51	0.79	1.03	2.05	2.15	1.66	0.69	0.71	0.93	1.02
T_1^{mFe}, 10^{-6} s	0.04	1.29	1.03	0.83	0.83	0.58	0.27	0.31	0.31	0.25	0.16
T_2^{Pa}, 10^{-8} s	3.78	2.44	2.63	2.68	2.89	2.85	2.94	3.09	3.34	3.35	2.74
T_2^{mFb}, 10^{-8} s	5.72	3.59	3.91	4.02	4.10	4.11	3.86	2.86	2.61	2.72	2.84
A, 10^5	49	66	34	21	7.6	6.3	2.1	0.78	0.82	1.9	47

[a] Determined for polarons $P^{\bullet+}$.
[b] Determined for methanofullerene anion radicals $mF^{\bullet-}$.
[c] Determined for immobilized polarons $P_{loc}^{\bullet+}$.
[d] Determined for immobilized methanofullerene anion radicals $mF_{loc}^{\bullet-}$.
[e] Determined for mobile methanofullerene anion radicals $mF_{mob}^{\bullet-}$.

originated due to IR irradiation from different warm electronic elements inside EPR spectrometer. Besides, the number of photons absorbed by polymer:fullerene system does not correlate with an effective number of spins initiated by these photons.

Once the temperature of the composite rises, the number of spin charge carriers decreases as it shown in Fig. 2b. Such spin decay can be explained in terms of its recombination with opposite charge carrier during polaron quasi-one-dimensional (Q1D) motion. When such carrier diffuses in polymer backbone between initial i and final j sites it spends the energy ΔE_{ij}. This is followed by its recombination with opposite charge on fullerene globe. Therefore, the decay of both spin charge carriers should follow the Miller–Abrahams energy-dependent equation [37]

$$N(\Delta E_{ij}) = N_0 \exp\left(\frac{\Delta E_{ij}}{k_B T}\right), \tag{1}$$

where k_B is the Boltzmann constant. It is seen from Fig. 2b that the dependences calculated from Eq. (1) with $\Delta E_{ij} = 0.002$, 0.012 and 0.015 eV fit well to the experimental data obtained for the $P_{loc}^{\bullet+}$, $mF_{loc}^{\bullet-}$ and $P_{mob}^{\bullet+} - mF_{loc}^{\bullet-}$ charge carriers, respectively. Pandey et al. have shown [38] that the charge is transferred through PCDTBT:PC$_{71}$BM BHJ mainly by holes. This fact may explain the higher value of ΔE_{ij} obtained for the opposite charge carriers.

3.3. LEPR line width

Various static and dynamics factors can affect a line width of paramagnetic centers. One of them is the above mentioned hyperfine interaction of the spins and the nuclei of heteroatoms included in the composite backbone. Interaction of polarons and methanofullerene ion radicals with other spins should also accelerate electron relaxation of all spin reservoirs and, therefore, broaden their EPR lines. Translational dynamics of polarons and reorientational diffusion of fullerene cage in BHJ should be also taken into account. If a part of charge carriers is partly fixed in spin traps formed in polymer matrix an effective line width should be also changed. The line widths of both charge carriers photoinduced in the PCDTBT:PC$_{71}$BM BHJ by photons of different energy at $T = 77$ K are summarized in Table 1. The analysis of the data presented allows concluding the notable monotonic line broadening with increasing photon energy. So, the number and depth of such traps are indeed governed by the energy of phonons initiating their formation.

A polaron $P_{mob}^{\bullet+}$ hopping along the polymer chain with the rate ν_{hop} can interact with unpaired electrons of methanofullerene anion radicals, quasi-rotating or captured by the spin traps, considering as more fixed centers as compared with diffusing polarons. This process should additionally broaden individual line by the value [39]

$$\delta(\Delta\omega) = \frac{\alpha^2 \nu_{hop} n_i}{2(1 + \alpha^2)}, \tag{2}$$

where $\alpha = (3/2) 2\pi J / h\nu_{hop}$, J is the constant of exchange interaction of spins in a radical pair, h is the Plank constant, $\nu_{hop} = \nu_{hop}^{(0)} \exp(-E_a/k_B T)$, E_a is the activation of polaron motion along polymer chain, and n_i is a number of radicals per polymer unit. The latter parameter is temperature dependent that should be taken into account for interpretation of experimental LEPR spectra. Weak and strong exchange limits can be realized in such multispin system. In the case of weak or strong exchange, the increase of ν_{hop} may result in the decrease or the increase in exchange frequency, respectively.

Isotropic widths of both contributions into an effective LEPR spectrum of the PCDTBT:PC$_{71}$BM composite and those normalized to the respective spin concentration per polymer unit n_i are shown in Fig. 3 as a function of temperature. The dependences calculated from Eq. (2) with $E_a = 0.008$ and 0.009 eV are also shown in the insert of Fig. 3. The data presented evidence the applicability of the approach proposed above for interpretation of electronic processes realized in the composite under study. It is seen from the Figure that the line width of polarons and methanofullerene anion radicals depends differently on the temperature compare to the case of the PCDTBT:PC$_{61}$BM BHJ [27]. It can be due to the different nature and mechanism of motion of spin charge carriers in domains inhomogeneously distributed in the composite under study. Such inhomogeneity seems to be more characteristic for methanofullerene cages than for polaronic phase due to possibly more ordered, layer morphology of polymer matrix of the composite. This is also evidenced by the difference in activation energy obtained for these charge carriers. An opposite temperature dependence of line width obtained for these charge carriers can be explained by their different interaction with microenvironment shifting spin–spin exchange interaction regime within the above mentioned weak and strong limits as it is realized in other similar systems [15,40]. The energies E_a necessary to activate the motion of polaronic and methanofullerene charge carriers in the PCDTBT:PC$_{71}$BM BHJ were appeared to be considerably smaller than those (0.028 and 0.013 eV, respectively) obtained for the PCDTBT:PC$_{61}$BM composite at the same experimental conditions [27]. This is additional evidence of a more ordered structure of the composite under study.
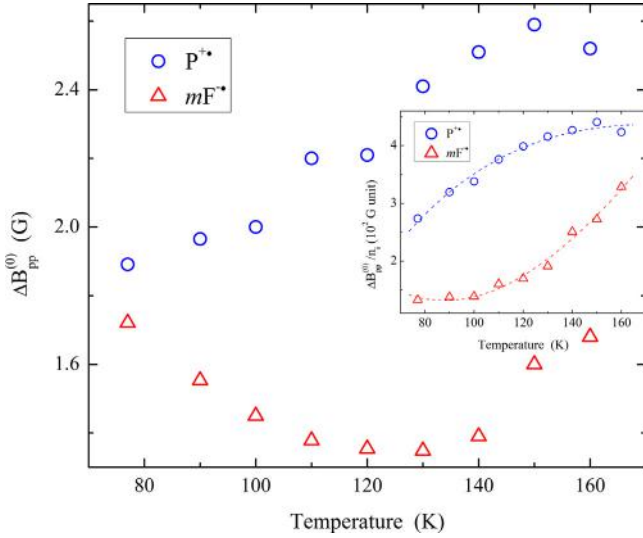
Fig. 3. Temperature dependence of the effective peak-to-peak line width $\Delta B_{pp}^{(0)}$ determined for the polarons $P^{\bullet+}$ (circles) and methanofullerene anion radicals $mF_{71}^{\bullet-}$ (triangles) photoinduced in the PCDTBT:PC$_{71}$BM composite by photons of white light with $T_c = 5500$ K. The upper (0) symbol in $\Delta B_{pp}^{(0)}$ means that this parameter is measured far from the spectrum microwave saturation. The same values divided by the number of appropriate charge carriers per a polymer unit, $\Delta B_{pp}^{(0)}/n_i$, are shown as function of temperature. The dependences calculated from Eq. (2) with $\nu_{hop}^{(0)} = 2.9 \times 10^7$ s^{-1}, $E_a = 0.008$ eV and $\nu_{hop}^{(0)} = 3.3 \times 10^7$ s^{-1}, $E_a = 0.009$ eV are shown by the top and bottom dashed lines. The error margins do not exceed the symbol size.

3.4. Spin relaxation and dynamics

At the increase of magnetic term B_1 of MW field the intensity of LEPR spectra of polarons and methanofullerene anion radicals photoinitiated in the PCDTBT:PC$_{71}$BM BHJ first increases linearly, reaching plateaus at some B_1 value and then decreases due to manifestation of a MW saturation effect [29]. As in the case of other spin solids, this allowed us to determine separately the spin-lattice T_1 and spin–spin T_2 relaxation times of these paramagnetic centers at wide regions of the temperature and photon energy $h\nu_{ph}$. Relaxation times obtained for charge carriers photoinduced in the system under study at different $h\nu_{ph}$ and $T = 77$ K are summarized in Table 1.

By the analysis of the data obtained one can conclude that the spin-lattice relaxation of charge carriers $P_{loc}^{\bullet+}$ and $mF_{mob}^{\bullet-}$ accelerates rather monotonically with the increase of $h\nu_{ph}$. The interaction of immobilized polaron with environments, however, decreases at $h\nu_{ph} = 2.73$ eV. The same relaxation parameter of $mF_{loc}^{\bullet-}$ increases remarkably only at $h\nu_{ph} \approx 1.9$–2.1 eV changing weakly at the lower and higher photon energy. All the centers demonstrate weak $T_2(h\nu_{ph})$ dependence within all the energy region used (see Table 1). The temperature also slightly affects spin–spin relaxation of all spin packets (not presented). The T_1 value of immobilized polarons changes weakly within the temperature range 77–160 K. On the other hand, an opposite charge carriers are characterized by much faster energy exchange with environment which accelerate their spin-lattice relaxation. The heating of the composite additionally steps up such exchange of $mF_{loc}^{\bullet-}$.

Spin relaxation is governed not only by the structure and morphology of the system but also by various spin-aided dynamics processes occurring in the PCDTBT:PC$_{71}$BM BHJ, e.g. the polaron diffusion along Q1D and quasi-three-dimensional (Q3D) diffusion between polymer chains with coefficients D_{1D} and D_{3D}, respectively, and pseudo-rotating libration of methanofullerene anion

radicals near own main molecular axis with coefficient D_{rot}. These processes induce an additional magnetic field in the vicinity of electron and nuclear spins and, therefore, accelerate electron relaxation of all spin ensembles. So, the following equations can be written for spin-lattice and spin–spin relaxation rates [41]:

$$T_1^{-1} = \langle \Delta\omega^2 \rangle [2J(\omega_e) + 8J(2\omega_e)], \tag{3}$$

$$T_2^{-1} = \langle \Delta\omega^2 \rangle [3J(0) + 5J(\omega_e) + 2J(2\omega_e)], \tag{4}$$

where $\langle \omega^2 \rangle = 1/10\gamma_e^4\hbar^2 S(S+1)n\Sigma_{ij}$ is a constant of a dipole–dipole interaction for a powder with the lattice sum Σ_{ij}, γ_e is gyromagnetic ratio for electron, $\hbar = h/2\pi$. $n_i = n_{loc} + n_{mob}/\sqrt{2}$ is the probability of localized, n_{loc}, and mobile, n_{mob}, spin situation on a lattice unit, $J(\omega_e) = (2D_{1D}^{|}\omega_e)^{-1/2}$ at $D_{1D}^{|} \gg \omega_e \gg D_{3D}$ or $J(0) = (2D_{1D}^{|}D_{3D})^{-1/2}$ at $D_{3D} \gg \omega_e$ is a spectral density function for Q1D motion, $D_{1D}^{|} = 4D_{1D}/L^2$, ω_e is the resonant angular frequency of electron spin precession, and L is the spatial extent of the polaron wave function equivalent approximately 3 units for PCDTBT [18]. Spectral density function for rotational librations with correlation time τ_c is $J(\omega_e) = 2\tau_c/(1 + \tau_c^2\omega_e^2)$.

Spin diffusion coefficients calculated from Eqs. (3) and (4) for charge carriers photoinduced in the PCDTBT:PC$_{71}$BM composite using appropriate spin concentration and relaxation data, as well as the spectral density functions are presented in Fig. 4a as a function of the initiated photon energy $h\nu_{ph}$. The Figure shows that the rates of polaron diffusion along and between polymer chains are governed by the energy of photons demonstrating extreme dependences with characteristic $h\nu_{ph} \approx 2.4$ eV. Dynamics parameter of methanofullerene anion radicals also extremely depends on the photon energy with characteristic $h\nu_{ph} \approx 1.8$ eV. This value lies near the band gap of the PCDTBT matrix, 1.88 eV [5]. It is seen from Table 1 that the anisotropy of polaron dynamics, $A = D_{1D}/D_{3D}$, in the PCDTBT:PC$_{71}$BM composite decreases nearly exponentially with the increase of $h\nu_{ph}$ up to 2.5 eV without an extremum at 2.1 eV characteristic for PCDTBT:PC$_{61}$BM BHJ [27]. This evidences more ordered BHJ under study at wider intermediate $h\nu_{ph}$ region. Similar strong decrease in the anisotropy of polaron dynamics was registered in the study of charge transfer in MW-treated P3HT:PC$_{61}$BM composite [42]. This effect was explained by more ordered polymer matrix and methanofullerene clusters in so modified system that facilitates polaron diffusion, inhibits fullerene reorientation and decreases interaction of charge carriers in photoinduced radical quasi-pairs. The formation of appropriate crystallites in an amorphous polymer matrix extends a diffusion of charge carriers and increases in efficiency of light conversion.

Dynamics parameters of charge carriers photoinduced by wide-range white ($T_c = 5500$ K) light are presented in Fig. 4b as a function of the temperature. Stronger temperature dependence characteristic for intrachain polaron dynamics can be described, e.g., in terms of polaron scattering on the phonons of crystalline lattice domains embedded into an amorphous polymer matrix [43]. According to this model, such scattering should accelerate polaron intrachain diffusion by the value

$$D_{1D}(T) = D_{1D}^{(0)}T^2 \cdot \left[\sinh\left(\frac{E_{ph}}{k_BT}\right) - 1\right], \tag{5}$$

where E_{ph} is the energy of lattice phonons. Indeed, it is seen from Fig. 4b, where dependence calculated from Eq. (5) with $E_{ph} = 0.124$ eV is also presented, that this approach satisfactorily describes the experimental data obtained. The latter value lies near the energy of lattice phonons of various conjugated polymers (0.09–0.32 eV) [44] and plastic solar cells [15], however, is sufficiently smaller
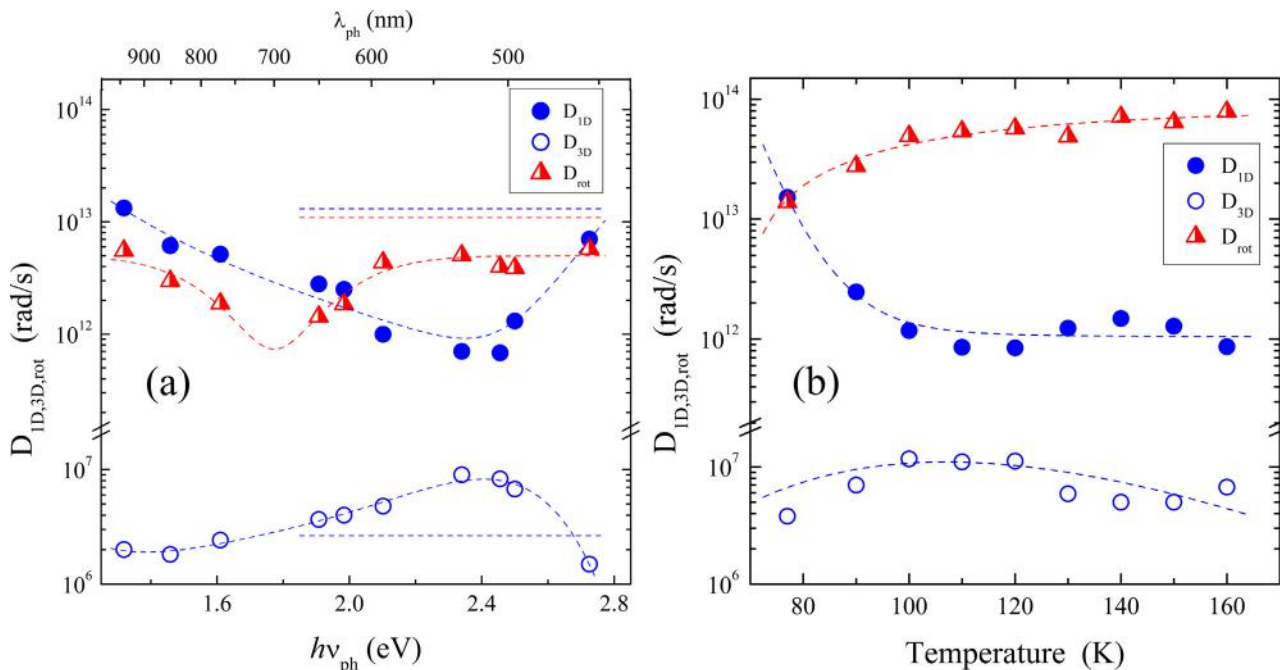
Fig. 4. (a) The coefficients of intrachain (D_{1D}, filled points) and interchain (D_{3D}, filled points) translative polaron $P^{\bullet+}_{mob}$ diffusion as well as librative quasi-rotation (D_{rot}, semi-filled points) of the methanofullerene anion radicals $mF^{\bullet-}_{mob}$ determined for the PCDTBT:PC$_{71}$BM composite at different photon energy/wavelength $h\nu_{ph}/\lambda_{ph}$ and $T = 77$ K. Respective values determined for these centers initiated in the system by polychromaic white light with color temperature $T_c = 5500$ K are shown by horizontal top, botton and middle dashed sectors, respectively. Dashed lines connect experimental points only for illustration to guide the eye. (b) Temperature dependence of the above charge carriers parameters determined upon illumination of the PCDTBT:PC$_{71}$BM composite by white light with $T_c = 5500$ K. Top-to-bottom dashed lines show the dependences calculated from Eq. (7) with $\omega^{(0)}_{rot} = 8.3 \times 10^{12}$ rad s^{-1} eV and $E_t = 0.010$ eV, Eq. (5) with $D^{(0)}_{1D} = 36.3$ rad s^{-1} K^{-1} and $E_{ph} = 0.124$ eV, and Eq. (6) with $D^{(0)}_{3D} = 0.44$ s^{-1} K^{-2}, $\omega_e = 6.1 \times 10^{10}$ rad s^{-1}, and $E_b = 0.072$ eV.

than evaluated for polaron dynamics in the PCDTBT:PC$_{61}$BM BHJ [27].

Spin charge carriers in polymer systems might be expected to have a large effect on their *ac* mobility [45], so, as in case of conducting polymers [46] and polymer:fullerene composites [15], the interchain spin dynamics in the PCDTBT:PC$_{71}$BM BHJ can be explained in the frames of the Pike [47] and Elliott [48] models based on the carrier hopping over the energetic barrier E_b. Such approach predicts the frequency and temperature dependent intrachain diffusion coefficient of polaron charge carriers

$$D_{3D}(\omega_e T) = D^{(0)}_{3D} k_1 T^2 \omega^s_e \exp\left(\frac{E_b}{k_B T}\right),$$ (6)

where k_1 is constant and $s = 1 - 6k_B T/E_b$ is the parameter reflecting polymer system dimensionality. As Fig. 4b evidences, this parameter indeed follows Eq. (6) with $E_b = 0.072$ eV at $\omega_e = 6.1 \times 10^{10}$ rad s^{-1}. It should be noted that the E_b obtained is nearly the same (0.079 eV) as necessary for polaron interchain diffusion in this matrix modified by PC$_{61}$BM [27].

Libration mobility of the PC$_{71}$BM cages can possibly be described in the framework of a semiclassical Marcus theory adopted for conjugated polymers [49]. According to this approach, methanofullerene ion radicals should reorient between polymer layers with the rate of

$$\omega_{rot} = \omega^{(0)}_{rot} \frac{1}{\sqrt{4E_r k_B T}} \exp\left(-\frac{E_r}{4k_B T}\right),$$ (7)

where E_r is both the inner- and outer-sphere reorganization energy of charge carriers due to their interaction with the lattice phonons. Indeed, such dynamics of the PC$_{71}$BM cages is realized according to the Marcus theory with $E_r = 0.010$ eV (Fig. 4b). This parameter is considerably lower than that obtained for the PCDTBT:PC$_{61}$BM BHJ

[27] due to a layered morphology of the composite under study, however, it lies near that determined for activation of reorientation of PC$_{61}$BM anion radicals in poly(3-alkylthiophenes) [26] as well as C$_{60}$- and C$_{70}$-anions in polymethylmethacrylate and cyclohexane [50]. Fullerene reorientational hopping or rotation in pure C$_{60}$ requires much higher activation energy (0.224 eV) [51], so, the interaction of such charge carriers with the nearest spins, lattice phonons, *etc.*, may affect their relaxation and dynamics and that should be taken into account when interpreting the results. Therefore, one may to conclude that the energy conversion by BHJ with PCDTBT matrix is realized within the visible and infrared regions of the sun spectrum with comparable quantum efficiency. The use of PC$_{71}$BM counter-ion instead of PC$_{61}$BM one leads to the deeper overlapping of molecular orbitals in polymer backbone. As a result, this leads to the layered morphology and more ordered PCDTBT:PC$_{71}$BM composite, hinders the formation of spin traps in its matrix and accelerates relaxation and dynamics of charge carriers. This significantly extends the scope of respective energy conversion elements.

4. Conclusions

In summary, we have presented the first results of the comprehensive LEPR study of photoinitiation, relaxation and dynamics of polarons diffusing along and between polymer chains and methanofullerene anion radicals librating between polymer lies of PCDTBT:PC$_{71}$BM composite. These processes are governed by the interaction of charge carriers with own microenvironment and other spin ensembles. The light photons also initiate spin traps in the polymer backbone which capture the part of these charge carriers. The number and depth of such traps are governed by the energy of photons. This originates the spin- and trap-assistance of

all main magnetic resonance, recombination, relaxation and dynamics processes carrying out in the PCDTBT:PC$_{71}$BM composite. The use of C$_{70}$-cage instead of C$_{60}$-globe as an electron acceptor accelerates own pseudo-rotation, and electron relaxation. It also deepens overlapping of molecular orbitals in appropriate BHJ. This hinders the formation of spin traps and provokes the more ordered (crystalline) structure of the PCDTBT:PC$_{71}$BM BHJ with the layered morphology accelerating spin and charge transport through BHJ. Such composite converses energy of photons of visible light and infrared irradiation into spin charge carriers that significantly extends the scope of energy conversion of such cells. The method can be efficiently used for respective detailed study of similar organic composites with low-band gap matrices for further creation of novel elements of organic electronics and spintronics.

Acknowledgments

References

[1] N.S. Sariciftci, L. Smilowitz, A.J. Heeger, F. Wudl, Science 258 (1992) 1474–1476.
[2] 2 ed., C. Brabec, U. Scherf, V. Dyakonov (Eds.), Organic Photovoltaics: Materials, Device Physics, and Manufacturing Technologies, vol. 1, Wiley-VCH, Weinheim, 2014.
[3] Y. Kim, S. Cook, S.M. Tuladhar, S.A. Choulis, J. Nelson, J.R. Durrant, D.D.C. Bradley, M. Giles, I. McCulloch, C.S. Ha, M. Ree, Nature Mater. 5 (2006) 197–203.
[4] (a) N. Blouin, A. Michaud, D. Gendron, S. Wakim, E. Blair, R. Neagu-Plesu, M. Belletete, G. Durocher, Y. Tao, M. Leclerc, J. Am. Chem. Soc. 130 (2008) 732–742;
(b) S. Wakim, S. Beaupre, N. Blouin, B.R. Aich, S. Rodman, R. Gaudiana, Y. Tao, M. Leclerc, J. Mater. Chem. 19 (2009) 5351–5358.
[5] J. Kim, M.H. Yun, G.H. Kim, J.Y. Kim, C. Yang, Polym. Chem. 3 (2012) 3276–3281.
[6] N. Blouin, A. Michaud, M. Leclerc, Adv. Mater. 19 (2007) 2295–2300.
[7] (a) M. Ito, K. Santhakumar, P. Kumar, K. Kojima, P.K. Shin, S. Ochiai, in: Z.H. Kafafi, C.J. Brabec, P.A. Lane (Eds.), Organic Photovoltaics XIII, vol. 84772012, pp. 19;
(b) Organic Solar Cells: Materials and Device Physics, in: W.C.H. Choy (Ed.), Springer, 2013;
(c) O. Ostroverkhova (Ed.), Handbook of Organic Materials for Optical and (Opto) Electronic Devices: Properties and Applications, vol. 39, Elsevier, 2013;
(d) Y.H. Huh, B. Park, Opt. Expr. 21 (2013) A146–A156.
[8] (a) D.H. Wang, J.H. Kim, I. Park, B.H. Hong, J.H. Park, A.J. Heeger, Angew. Chem. Int. Ed. 52 (2013) 2874–2880;
(b) J. Griffin, A.J. Pearson, N.W. Scarratt, T. Wang, A.D.F. Dunbar, H. Yi, A. Iraqi, A.R. Buckley, D.G. Lidzey, Org. Electron. 21 (2015) 216–222.
[9] M.M. Wienk, J.M. Kroon, W.J.H. Verhees, J. Knol, J.C. Hummelen, P.A. van Hal, R.A.J. Janssen, Angew. Chem. Int. Ed. 42 (2003) 3371–3375.
[10] C. Schlenker, M.E. Thompson, in: R.M. Metzger (Ed.), Unimolecular and Supramolecular Electronics I, vol. 312, Springer, Berlin/Heidelberg, 2012, pp. 175–212.
[11] N. Banerji, S. Cowan, M. Leclerc, E. Vauthey, A.J. Heeger, J. Am. Chem. Soc. 132 (2010) 17459–17470.
[12] (a) J.S. Moon, J. Jo, A.J. Heeger, Adv. Energy Mater. 2 (2012) 304–308;
(b) X.H. Lu, H. Hlaing, D.S. Germack, J. Peet, W.H. Jo, D. Andrienko, K. Kremer, B.M. Ocko, Nat. Commun. 3 (2012), doi:http://dx.doi.org/10.1038/ncomms1790.
[13] R. Gutzler, D.F. Perepichka, J. Am. Chem. Soc. 135 (2013) 16585–16594.
[14] (a) R.A.J. Janssen, D. Moses, N.S. Sariciftci, J. Chem. Phys. 101 (1994) 9519–9527;
(b) S. Sensfuss, A. Konkin, H.K. Roth, M. Al-Ibrahim, U. Zhokhavets, V.I. Gobsch, G.A. Krinichnyi, E. Klemm, Synth. Met. 137 (2003) 1433–1434.
[15] V.I. Krinichnyi, Encyclopedia of Polymer Composites: Properties, Performance and Applications, in: M. Lechkov, S. Prandzheva (Eds.), Nova Science Publishers, Hauppauge, New York, 2009, pp. 417–446 Ch. 11.
[16] (a) J. De Ceuster, E. Goovaerts, A. Bouwen, J.C. Hummelen, V. Dyakonov, Phys. Rev. B 64 (2001) 195206/01–195206/06;
(b) A. Aguirre, P. Gast, S. Orlinskii, I. Akimoto, E.J.J. Groenen, H. El Mkami, E. Goovaerts, S. Van Doorslaer, Phys. Chem. Chem. Phys. 10 (2008) 7129–7138.
[17] O.G. Poluektov, S. Filippone, N. Martín, A. Sperlich, C. Deibel, V. Dyakonov, J. Phys. Chem. B 114 (2010) 14426–14429.
[18] J. Niklas, K.L. Mardis, B.P. Banks, G.M. Grooms, A. Sperlich, V. Dyakonov, S. Beauprë, M. Leclerc, T. Xu, L. Yue, O.G. Poluektov, Phys. Chem. Chem. Phys. 15 (2013) 9562–9574.
[19] V. Dyakonov, G. Zoriniants, M. Scharber, C.J. Brabec, R.A.J. Janssen, J.C. Hummelen, N.S. Sariciftci, Phys. Rev. B 59 (1999) 8019–8025.
[20] (a) M. Pientka, J. Wisch, S. Boger, J. Parisi, V. Dyakonov, A. Rogach, D. Talapin, H. Weller, Thin Solid Films 451–452 (2004) 48–53;
(b) M. Pientka, V. Dyakonov, D. Meissner, A. Rogach, D. Vanderzande, H. Weller, L. Lutsen, Nanotechnology 15 (2004) 163–170.
[21] J.M. Lupton, D.R. McCamey, C. Boehme, Chem. Phys. Chem. 11 (2010) 3040–3058.
[22] D.R. McCamey, K.J. van Schooten, W.J. Baker, S.Y. Lee, S.-Y. Paik, J.M. Lupton, C. Boehme, Phys. Rev. Lett. 104 (2010) 017601–017604.
[23] V.I. Krinichnyi, E.I. Yudanova, AIP Adv. 1 (2011) 22131/01–22131/15.
[24] V.I. Krinichnyi, E.I. Yudanova, J. Phys. Chem. C 116 (2012) 9189–9195.
[25] V.I. Krinichnyi, Sol. Energy Mater. Sol. Cells 92 (2008) 942–948.
[26] V.I. Krinichnyi, E.I. Yudanova, N.G. Spitsina, J. Phys. Chem. C 114 (2010) 16756–16766.
[27] V.I. Krinichnyi, E.I. Yudanova, N.N. Denisov, J. Chem. Phys. 141 (2014) 44906/01–44906/11.
[28] M.H. Tong, N.E. Coates, D. Moses, A.J. Heeger, S. Beaupre, M. Leclerc, Phys. Rev. B 81 (2010) 125210–125215.
[29] C.P. Poole, Electron spin resonance, A comprehensive treatise on experimental techniques, John Wiley & Sons, New York, 1983.
[30] (a) H.K. Roth, V.I. Krinichnyi, Synth. Met. 137 (2003) 1431–1432;
(b) V.I. Krinichnyi, H.K. Roth, A.L. Konkin, Phys. B 344 (2004) 430–435.
[31] V.I. Krinichnyi, E.I. Yudanova, Sol. Energy Mater. Sol. Cells 95 (2011) 2302–2313.
[32] (a) B. Kraabel, D. McBranch, N.S. Sariciftci, D. Moses, A.J. Heeger, Phys. Rev. B 50 (1994) 18543–18552;
(b) C.J. Brabec, G. Zerza, G. Cerullo, S. DeSilvestri, S. Luzatti, J.C. Hummelen, N.S. Sariciftci, Chem. Phys. Lett. 340 (2001) 232–236.
[33] B. Yan, N.A. Schultz, A.L. Efros, P.C. Taylor, Phys. Rev. Lett. 84 (2000) 4180–4183.
[34] M. Westerling, R. Osterbacka, H. Stubb, Phys. Rev. B 66 (2002) 165220/01–165220/07.
[35] M.D. Heinemann, K. von Maydell, F. Zutz, J. Kolny-Olesiak, H. Borchert, I. Riedel, J. Parisi, Adv. Funct. Mater. 19 (2009) 3788–3795.
[36] S.H. Park, A. Roy, S. Beaupre, S. Cho, N. Coates, J.S. Moon, D. Moses, M. Leclerc, K. Lee, A.J. Heeger, Nat. Photonics 3 (2009) 297–302.
[37] J. Nelson, Phys. Rev. B 67 (2003) 155209/01–155209/10.
[38] A.K. Pandey, M. Aljada, A. Pivrikas, M. Velusamy, P.L. Burn, P. Meredith, E.B. Namdas, ACS Photonics 1 (2014) 114–120.
[39] Y.N. Molin, K.M. Salikhov, K.I. Zamaraev, Spin Exchange, Springer, Berlin, 1980.
[40] V.I. Krinichnyi, Appl. Phys. Rev. 1 (2014) 21305/01–021305/40.
[41] F. Carrington, A.D. McLachlan, Introduction to Magnetic Resonance with Application to Chemistry and Chemical Physics, Harrer & Row, Publishers, New York, Evanston, London, 1967.
[42] E.I. Yudanova, V.I. Krinichnyi, Polym. Sci. Ser. A 55 (2013) 233–243.
[43] S. Kivelson, A.J. Heeger, Synth. Met. 22 (1988) 371–384.
[44] V.I. Krinichnyi, Synth. Met. 108 (2000) 173–222.
[45] J. Kočka, S.R. Elliott, E.A. Davis, J. Phys. C Solid State Phys. 12 (1979) 2589–2596.
[46] (a) J.P. Parneix, M. El Kadiri, in: H. Kuzmany, M. Mehring, S. Roth (Eds.), Electronic Properties of Conjugated Polymers, vol. 76, Springer-Verlag, Berlin, 1987, pp. 23–26;
(b) V.I. Krinichnyi, in: S. Schlick (Ed.), Advanced ESR Methods in Polymer Research, Wiley, Hoboken, NJ, 2006, pp. 307–338 Ch. 12.
[47] G.E. Pike, Phys. Rev. B 6 (1972) 1572–1580.
[48] S.R. Elliott, Solid State Commun. 28 (1978) 939–942.
[49] (a) A. Van Vooren, J.-S. Kim, J. Cornil, Eur. J. Chem. Phys. Phys. Chem. 9 (2008) 989–993;
(b) Y.-K. Lan, C.-I. Huang, J. Phys. Chem. B 112 (2008) 14857–14862.
[50] G. Agostini, C. Corvaja, L. Pasimeni, Chem. Phys. 202 (1996) 349–356.
[51] B. Morosin, Z.B. Hu, J.D. Jorgensen, S. Short, J.E. Schirber, G.H. Kwei, Phys. Rev. B 59 (1999) 6051–6057.